Preprint Title	**Stability analysis of heat transfer in nanomaterial flow of boundary layer towards a shrinking surface: Hybrid nanofluid versus nanofluid**
Authors	Aqeel u. Rehman and Zaheer Abbas
Publication Date	15 Dez. 2021
Article Type	Full Research Paper
ORCID® iDs	Zaheer Abbas - https://orcid.org/0000-0002-1300-7098

Stability analysis of heat transfer in nanomaterial flow of boundary layer towards a shrinking surface: Hybrid nanofluid versus nanofluid

Aqeel ur Rehman and Zaheer Abbas[1]

Department of Mathematics, The Islamia University of Bahawalpur,
Bahawalpur 63100, Pakistan

Abstract: Many boundary value problems (BVPs) have dual solutions in some cases containing one stable solution (upper branch) while other unstable (lower branch). In this paper, MHD flow and heat transfer past a shrinking sheet is studied for three distinct fluids: $Al_2O_3 - ZnO$ / kerosene hybrid nanofluid, Al_2O_3 / kerosene nanofluid, and ZnO / kerosene nanofluid. The partial differential equations (PDEs) are turned into ordinary differential equations (ODEs) using an appropriate transformation and then dual solutions are obtained analytically by employing the Least Square method (LSM). Moreover, stability analysis is implemented on the time-dependent case by calculating the least eigenvalues using Matlab routine bvp4c. It is noticed that negative eigenvalue is related to unstable solution i.e., it provides initial progress of disturbance and positive eigenvalue is related to stable solution i.e., the disturbance in solution decline initially. The impacts of various parameters, skin friction coefficient, and local Nusselt number for dual solutions are presented graphically. It is also noted that the results obtained for hybrid nanofluids are better than ordinary nanofluids.

Keywords: Stability analysis; hybrid nanofluid; shrinking sheet; dual solutions; analytical procedure.

NOMENCLATURE			
f, θ, F, G	Functions in dimensionless form	q_w, q_r	Heat flux at the lower plate and radiative heat flux
$\tilde{u}, \tilde{v}$	Components of velocity in $\tilde{x}$ and $\tilde{y}$ directions, respectively.	**Greek Symbols**	

[1]Corresponding author.

e-mail address: za_qau@yahoo.com (Z. Abbas)

T	Temperature function	γ	Eigenvalue parameter
T_w, T_∞	Wall and ambient temperature, respectively	τ	Time parameter
B_0	Strength of magnetic field	λ	Velocity ratio parameter
$Nu_{\tilde{x}}$	Local Nusselt number	η	Similarity variable
C_p	Specific heat at constant pressure	ϕ	Volume fraction of nanoparticle
a	Stretching/shrinking velocity constant	ρ	Density
b	Free stream velocity constant	σ	Electrical conductivity
A_{1-5}	Constants in dimensionless form	υ	Kinematic viscosity
C_f	Coefficient of skin friction	μ	Dynamic viscosity
$\tilde{R}_1, \tilde{R}_2$	Residuals	σ_1	Stefan–Boltzmann constant
W_{1-6}	Weight functions	k_1	Mean absorption coefficient
Re	Reynolds number	**Subscripts**	
k	Thermal conductivity	j	Indices for unknowns
P_r	Prandtl number	s_1, s_2	Solid-nanoparticles for Al_2O_3 and ZnO, respectively
R	Radiation parameter	f	Base fluid
M	Magnetic parameter	nf	Nanofluid
$\tilde{u}_e, \tilde{u}_w$	Free stream velocity, wall velocity	hnf	Hybrid nanofluid

1. Introduction

The remarkable analysis in the flow of boundary layer past a stretching/shrinking sheet has been completed by many specialists as it has vast uses in industries and engineering. Some common examples are packaging of products, manufacturing of polymers, glass blowing, drawing of wires and aerospace coatings, etc. The real behavior of the surface depends on the rate of stretching/shrinking and cooling (exchange of heat) during the process of stretching/shrinking. Miklavcic and Wang [1] initiated the flow of fluid caused by a shrinking sheet and presented

numerical, exact, and close form solutions and they obtained dual solutions for the case of the shrinking sheet. The analysis of the flow of stagnation point past a shrinking sheet was studied by Wang [2]. He found dual solutions by taking some range of velocity ratio parameters. Ishak et al. [3] made an extension on the work of Wang [2] by taking micropolar fluid and finding multiple solutions. The solution in the analytical form for the flow of boundary layer caused by a shrinking sheet was given by Fang and Zhang [4]. They studied the close form solutions with special parameters. The MHD flow of fluid near the region of stagnation point towards a shrinking sheet was discussed by Lok et al. [5]. The study of flow problems through a permeable shrinking surface in the region of stagnation point having dual solutions was presented by Bhattacharyya and Layek [6] and they evaluated numerical solution by examining the impacts of suction/blowing and radiation. The slip effects on the flow of stagnation point caused by shrinking sheet were presented by Bhattacharyya et al. [7]. They also established dual solutions by employing shooting techniques to solve self-similar equations and they also noticed the increment in the range of dual solutions with slip parameter. Few other researchers [8–10] also found the dual solutions for shrinking sheets by using several physical effects.

In the 19th century, Maxwell [11] studied the influence of fluid's thermal conductivity by taking various substances with improved conductivity. Latterly, to improve the fluid conductivity the idea of nanofluid as a new type of heat transfer fluid was given by Choi and Eastman [12]. They studied that nanofluid is formed when the nanoparticles are suspended in a base fluid. With the development in the process of nanotechnology-based transfer of heat, nanofluid is defined as a colloidal suspension of nanomaterials (1–100 nm) in a base fluid. By adding the nanoparticles like carbon material, metal oxides, and metals in base fluids, the outgrowth thermal conductivity of fluids increases in conventional heat transfer fluids and limits the ability of cooling. Nanofluids have vast applications in the manufacturing and engineering industries like fuel generators, cooling of electronics, and engine [13]. Therefore, nanofluids impact a great effort and interest to the researcher. Few other researchers have extended a great analysis of nanofluids [14–16].

In recent times, a new type of nanofluid called the hybrid nanofluid is introduced which is formed by suspension of assorted nanoparticles in the base fluid. Hybrid nanofluid enhances properties of heat transfer as well as provides extra substantial thermal, physical, and rheological features. This fluid captivated many researchers to extend the given problem for the transfer of heat. In this regard, an experimental analysis is conducted by Suresh et al. [17] on the synthesis,

characterization of $Al_2O_3 - Cu / H_2O$ nanocomposite powder by taking various percentages of volume concentrations. They determined the pH of nanofluids by studying the stability of nanofluids and found that the stability diminishes with increasing concentration of volume. Moreover, Suresh et al. [18] inspect the thermal and physical properties of $Al_2O_3 - Cu / H_2O$ hybrid nanofluid. They also showed that the reliability and efficiency of thermal conductivity are enhanced with $Al_2O_3 - Cu / H_2O$ hybrid nanofluid. The three-dimensional flow of $Al_2O_3 - Cu / H_2O$ a hybrid nanofluid past a stretching sheet with Lorentz force was numerically noticed by Devi and Devi [19]. Their findings reported that the optimal rate of heat transfer for hybrid nanofluid is gained by selecting different nanoparticles. Due to this regard, many investigators studied the hybrid nanofluids by taking physical assumptions over a stretching/shrinking sheet-like, Khashi'ie et al. [20], Zainal et al. [21], and Waini et al. [22].

In the last two or more decades, researchers started to apply a stability analysis on problems having multiple solutions. Some of them are stable and others are unstable. Due to the existence of dual solutions, stability analysis in fluid dynamics problems plays an important role and is roughly linked with some numerical errors. In this era, Merkin [23] was the first who perform stability analysis to check the stable solution. He calculated eigenvalues and obtained a stable solution for positive eigenvalues and an unstable solution for negative eigenvalues. Later, many researchers have done stability analysis for dual solutions in stretching/shrinking flows or mixed convection flows. The influences of transpiration on boundary layer flow towards surfaces in motion were discussed by Weidman et al. [24]. They found dual solutions and reported that the range of dual solutions decreases or increases by considering suction/blowing effects for zero transpiration. Within a porous media, an unsteady flow of mixed convection towards a vertical sheet near a region of stagnation point was discussed by Merill et al. [25]. They noticed dual solutions on large values of time by performing stability analysis and proved that the lower branch solution is unstable whereas the upper branch solution is stable. Later on, various researchers [26–32] have performed good analyses on stability and found multiple solutions. They reported in their study that the stable solutions are physically substantial and unstable solutions are not.

For the flow of boundary layer past a shrinking sheet with nonlinear differential equations, analytical solutions have a significant role. But in the case of strictly nonlinear coupled equations, it is very challenging work to find an analytical solution. In this regard, various analytical methods

have been employed to find estimated solutions to such nonlinear differential equations. The analytical outcomes of very weak nonlinear BVP were found by Nayfeh [33]. He used perturbation methods for this purpose but for a certain range of parameters, this method is not so efficient. The homotopy perturbation method was applied by Khan et al. [34] for the influence of thermal conductivity on the transfer of heat inside a hollow sphere with heat generation. Some other analytical techniques have also been employed for solving the nonlinear problems like linearization methods [35], Lindstedt–Poincare method [36], differential transformation method [37], and optimal homotopy perturbation method [38]. Moreover, some other simple and more accurate analytical methods are available for solving differential equations namely: weighted residual methods which consist of the Least square method, method of Moments, Collocation method, and Galerkin method. The least-square method was initiated by Bouaziz and Aziz [39]. They employed this method for predicting the longitudinal fin performance and found this method more simple and accurate than others. Furthermore, the detailed study on the Least square method was completed by Hatami and Ganji [40–42] and they employed this method on different problems of fluid mechanics.

The main focus of the present paper is to use an analytical method namely: Least square method to find the dual solutions of MHD flow and heat transfer past a shrinking sheet for three distinct fluids. Also to check the reliable solution using stability analysis and evaluate the corresponding eigenvalues for both solutions.

2. Mathematical model

Consider a two-dimensional flow of boundary layer and heat transfer for three different fluids near a region of stagnation point caused by stretching/shrinking surface. Aluminum oxide (Al_2O_3) and zinc oxide (ZnO) are chosen as the nanomaterials with Kerosene oil as the base fluid. The surface is placed along a horizontal axis and the vertical axis is considered normal to the surface as displayed in Fig. 1. The surface is stretched or shrunk having velocity $\tilde{u}_w(\tilde{x}) = a\tilde{x}$, here $a<0$ determines shrinking and $a>0$ determines stretching surface. For the orthogonal flow of stagnation point, fluid flow over the surface with velocity $\tilde{u}_e(\tilde{x}) = b\tilde{x}$ here $b>0$ determines the stagnation flow strength. An external magnetic field with strength B_0 is also taken in the normal

direction to the surface. Since it is an earlier assumption that the magnetic Reynolds number is too low, which causes the higher magnetic diffusion than magnetic advection, due to which induced magnetic field is ignored.

Under all assumptions stated above, the governing Navier–Stokes and energy equations for the case of steady flow with radiation are written as:

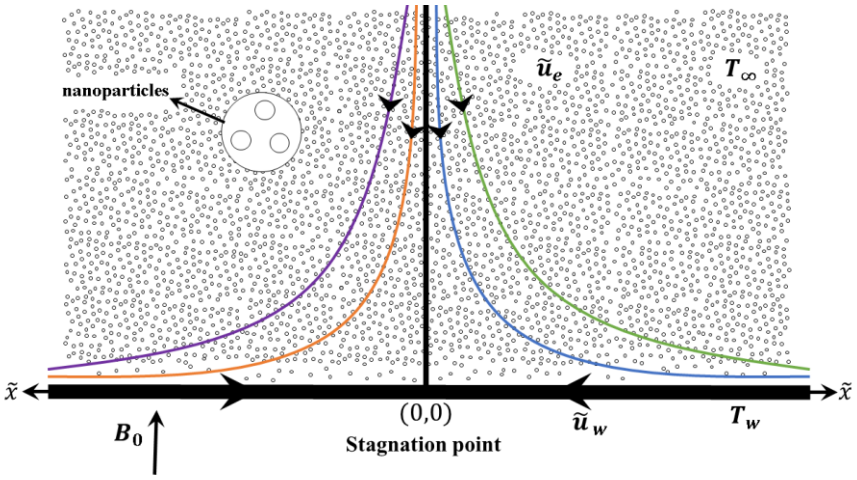

Fig. 1: Problem's geometry

$$\frac{\partial \tilde{u}}{\partial \tilde{x}}+\frac{\partial \tilde{v}}{\partial \tilde{y}}=0, \tag{1}$$

$$\tilde{u}\frac{\partial \tilde{u}}{\partial \tilde{x}}+\tilde{v}\frac{\partial \tilde{u}}{\partial \tilde{y}}=-\frac{1}{\rho_{hnf}}\tilde{u}_e\frac{d\tilde{u}_e}{d\tilde{x}}+\frac{\mu_{hnf}}{\rho_{hnf}}\frac{\partial^2\tilde{u}}{\partial\tilde{y}^2}+\frac{\sigma_{hnf}}{\rho_{hnf}}B_0^2\left(\tilde{u}_e-\tilde{u}\right), \tag{2}$$

$$\tilde{u}\frac{\partial T}{\partial \tilde{x}}+\tilde{v}\frac{\partial T}{\partial \tilde{y}}=\left(\frac{k}{\rho C_p}\right)_{hnf}\frac{\partial^2 T}{\partial\tilde{y}^2}-\frac{1}{(\rho C_p)_{hnf}}\frac{\partial q_r}{\partial\tilde{y}}, \tag{3}$$

here $\tilde{u}$ and $\tilde{v}$ denotes velocity components of fluid along the horizontal and vertical axis, respectively, and T indicates temperature. The subscripts hnf, nf and f indicate hybrid nanofluid, nanofluid, and base fluid respectively. Physical meanings of all other parameters are given in nomenclature.

Associated boundary conditions (BCs) are:

$$\begin{aligned} &\text{For}\quad \tilde{y}=0: \qquad \tilde{u}=\tilde{u}_w,\quad \tilde{v}=0,\quad T=T_w,\\ &\text{For}\quad \tilde{y}\to\infty: \qquad \tilde{u}\to 0,\quad \tilde{v}\to 0,\quad T\to T_\infty. \end{aligned} \tag{4}$$

Table 1: The physical and thermal properties of magnetic nanomaterials and base fluid [32]:

Materials	$\rho\ \left(kg/m^3\right)$	$\sigma\left((\Omega\cdot m)^{-1}\right)$	$k\left(W(mK)^{-1}\right)$	$C_p\left(J(kgK)^{-1}\right)$
Al_2O_3	3970	1×10^{-10}	40	765
ZnO	5700	$10-1\times10^{-3}$	25	523
kerosene oil	783	6×10^{-10}	0.15	2090

Table 2: The effective properties of nanofluid and hybrid nanofluid are defined below [32]:

	Nanofluid	Hybrid nanofluid
Dynamic viscosity	$\mu_{nf}=\frac{\mu_f}{\left(1-\phi_1\right)^{2.5}}$	$\mu_{hnf}=\frac{\mu_{nf}}{\left(1-\phi_2\right)^{2.5}}$
Density	$\rho_{nf}=\left(1-\phi_1\right)\rho_f+\rho_{s1}\phi_1$	$\rho_{hnf}=\left(1-\phi_2\right)\rho_{nf}+\rho_{s2}\phi_2$
Electrical conductivity	$\sigma_{nf}=\sigma_f\left(\frac{\sigma_{s1}\left(1+2\phi_1\right)+2\sigma_f\left(1-\phi_1\right)}{\sigma_{s1}\left(1-\phi_1\right)+\sigma_f\left(2+\phi_1\right)}\right)$	$\sigma_{hnf}=\sigma_{nf}\left(\frac{2\left(1-\phi_2\right)\sigma_f+\left(2\phi_2+1\right)\sigma_{s2}}{\left(\phi_2+2\right)\sigma_f+\left(1-\phi_2\right)\sigma_{s2}}\right)$
Thermal conductivity	$k_{nf}=k_f\left(\frac{2k_f+k_{s1}-2\left(k_f-k_{s1}\right)\phi_1}{2k_f+k_{s1}+\left(k_f-k_{s1}\right)\phi_1}\right)$	$k_{hnf}=k_{nf}\left(\frac{2k_{nf}+k_{s2}-2\left(k_{nf}-k_{s2}\right)\phi_2}{2k_{nf}+k_{s2}+\left(k_{nf}-k_{s2}\right)\phi_2}\right)$
Heat capacity	$(\rho C_p)_{nf}=(\rho C_p)_f(1-\phi_1)+(\rho C_p)_{s1}\phi_1$	$(\rho C_p)_{hnf}=(1-\phi_2)(\rho C_p)_{nf}+\phi_2(\rho C_p)_{s2}$

The radiative heat flux is denoted by q_r and is given by Rosseland approximation [43]:

$$q_r=-\frac{4\sigma_1}{3k_1}\frac{\partial T^4}{\partial\tilde{y}}.$$

The variation of temperature (T^4) is taken as Taylor's expansion, then ignoring the terms of higher-order and after that, the expansion of (T^4) about T_∞ gives $T^4\cong4T_\infty^3T-3T_\infty^4$ and

$$\frac{\partial q_r}{\partial\tilde{y}}=-\frac{16}{3}\frac{\sigma_1}{k_1}T_0^3\frac{\partial^2T}{\partial\tilde{y}^2}\ . \tag{5}$$

Eq. (3) then becomes

$$\tilde{u}\frac{\partial T}{\partial\tilde{x}}+\tilde{v}\frac{\partial T}{\partial\tilde{y}}=\frac{k_{hnf}}{(\rho C_p)_{hnf}}\frac{\partial^2T}{\partial\tilde{y}^2}+\frac{1}{(\rho C_p)_{hnf}}\frac{16\sigma_1T_0^3}{3k_1}\frac{\partial^2T}{\partial\tilde{y}^2}\ . \tag{6}$$

Now the similarity transformations are introduced in the following forms:

$$\tilde{u} = f'(\eta)\, b\tilde{x}, \quad \tilde{v} = -f(\eta)\sqrt{\upsilon_f\, b}, \quad \theta(\eta) = \frac{T - T_\infty}{T_w - T_\infty}, \quad \eta = \sqrt{\frac{b}{\upsilon_f}}\,\tilde{y}, \tag{7}$$

here prime specifies differentiation of function with respect to variable η. The dimensionless form of governing equations are presented as follows:

$$\frac{A_1}{A_2} f''' + 1 - f'^2 + f f'' + M\frac{A_3}{A_2}(1 - f') = 0, \tag{8}$$

$$\left(A_4 + R\right)\theta'' + A_5\, P_r\, f\, \theta' = 0, \tag{9}$$

where the magnetic number M, Prandtl number P_r and radiation parameter R are given as

$$M = \frac{\sigma_f\, B_0^2}{b\rho_f}, \; P_r = \left(\frac{\mu C_p}{k}\right)_f, R = \frac{16\,\sigma_1 T_\infty^3}{3\,k_1 k_f}. \tag{10}$$

And the constant parameters A_1, A_2, A_3, A_4 and A_5 are:

$$A_1 = \frac{\mu_{hnf}}{\mu_f}, \; A_2 = \frac{\rho_{hnf}}{\rho_f}, \; A_3 = \frac{\sigma_{hnf}}{\sigma_f}, \; A_4 = \frac{k_{hnf}}{k_f}, \; A_5 = \frac{(\rho C_p)_{hnf}}{(\rho C_p)_f}. \tag{11}$$

BCs:

$$\begin{aligned} &\text{For} \quad \eta = 0: \qquad f = 0, \quad f' = \lambda \quad \theta = 1, \\ &\text{For} \quad \eta \to \infty: \qquad f' \to 1, \qquad \theta \to 0. \end{aligned} \tag{12}$$

Here, $\lambda = \dfrac{a}{b}$ represents the velocity ratio parameter.

The physical terms of attention are coefficient of skin friction C_f and local Nusselt number Nu_x and both of them are given below:

$$Re_{\tilde{x}}^{1/2} C_f = A_1\, f''(0), \quad Re_{\tilde{x}}^{-1/2} Nu_{\tilde{x}} = -A_4\, \theta'(0), \tag{13}$$

here $Re_{\tilde{x}} = \tilde{u}_e \tilde{x}/\upsilon_f$ indicates the local Reynolds number.

3. Stability analysis

Stability analysis has been performed by many researchers like Awaludin et al. [28], Hamid et al. [29], and Waini et al. [30] to check the stable and unstable solutions. For this purpose, an additional dimensionless time variable $\tau = b\tilde{t}$ is considered, due to which the flow problem

becomes unsteady. Prandtl theory is utilized and pressure gradient is eliminated from component forms and then equations for unsteady flow are gained as

$$\frac{\partial \tilde{u}}{\partial \tilde{t}}+\tilde{u}\frac{\partial \tilde{u}}{\partial \tilde{x}}+\tilde{v}\frac{\partial \tilde{u}}{\partial \tilde{y}}=-\frac{1}{\rho_{hnf}}\tilde{u}_e\frac{d\tilde{u}_e}{d\tilde{x}}+\frac{\mu_{hnf}}{\rho_{hnf}}\frac{\partial^2\tilde{u}}{\partial\tilde{y}^2}+\frac{\sigma_{hnf}}{\rho_{hnf}}B_0^2\left(\tilde{u}_e-\tilde{u}\right), \tag{14}$$

$$\frac{\partial T}{\partial \tilde{t}}+\tilde{u}\frac{\partial T}{\partial \tilde{x}}+\tilde{v}\frac{\partial T}{\partial \tilde{y}}=\frac{k_{hnf}}{(\rho C_p)_{hnf}}\frac{\partial^2 T}{\partial\tilde{y}^2}+\frac{1}{(\rho C_p)_{hnf}}\frac{16\sigma_1 T_0^3}{3k_1}\frac{\partial^2 T}{\partial\tilde{y}^2}\ . \tag{15}$$

Now for a dimensionless form of the above equations, new transformations with time-variable τ are used as

$$\tilde{u}=f'(\eta,\tau)\,b\,\tilde{x},\ \tilde{v}=-f(\eta,\tau)\sqrt{\upsilon_f\, b}\,,\ \theta(\eta,\tau)=\frac{T-T_\infty}{T_w-T_\infty},\ \eta=\sqrt{\frac{b}{\upsilon_f}}\,\tilde{y},\ \tau=b\tilde{t}\,. \tag{16}$$

Using the above transformation (16) in Eqs. (14) and (15) gives

$$\frac{A_1}{A_2}\frac{\partial^3 f}{\partial\eta^3}+1-\left(\frac{\partial f}{\partial\eta}\right)^2+f\frac{\partial^2 f}{\partial\eta^2}+M\frac{A_3}{A_2}\left(1-\frac{\partial f}{\partial\eta}\right)-\frac{\partial^2 f}{\partial\eta\,\partial\tau}=0, \tag{17}$$

$$\left(A_4+R\right)\frac{\partial^2\theta}{\partial\eta^2}+A_5P_r f\frac{\partial\theta}{\partial\eta}-A_5P_r\frac{\partial\theta}{\partial\tau}=0, \tag{18}$$

and the associated boundary conditions in the case of unsteady flow are:

$$\begin{aligned}&\text{For}\quad \eta=0: && f(0,\tau)=0, && \frac{\partial f}{\partial\eta}(0,\tau)=\lambda, && \theta(0,\tau)=1,\\ &\text{For}\ \ \eta\to\infty: && \frac{\partial f}{\partial\eta}(\eta,\tau)\to 1, && && \theta(\eta,\tau)\to 0.\end{aligned} \tag{19}$$

Following Awaludin et al. [28], Hamid et al. [29] and Waini et al. [30], the unknown functions are:

$$\begin{aligned}f(\eta,\tau)&=f_0(\eta)+F(\eta,\tau)\,e^{-\gamma\tau},\\ \theta(\eta,\tau)&=\theta_0(\eta)+G(\eta,\tau)\,e^{-\gamma\tau}.\end{aligned} \tag{20}$$

Here, γ is the unidentified eigenvalue parameter, $f_0(\eta)$ and $\theta_0(\eta)$ are steady solutions of a problem given in Eqs. (8)−(9) and both are larger than the functions $F(\eta,\tau)$ and $G(\eta,\tau)$. Substituting Eq. (20) into Eqs. (17)−(18), the following linearized problem is obtained:

$$\frac{A_1}{A_2}\frac{\partial^3 F}{\partial\eta^3}+f_0\frac{\partial^2 F}{\partial\eta^2}+f_0''F-\left(2f_0'-\gamma\right)\frac{\partial F}{\partial\eta}-M\frac{A_3}{A_2}\frac{\partial F}{\partial\eta}-\frac{\partial^2 F}{\partial\eta\,\partial\tau}=0, \tag{21}$$

$$\left(A_4+R\right)\frac{\partial^2 G}{\partial \eta^2}+A_5 P_r\left(f_0\frac{\partial G}{\partial \eta}+F\,\theta_0'\ +\gamma G-\frac{\partial G}{\partial \tau}\right)=0\,, \tag{22}$$

along with BCs:

$$\begin{aligned}&\text{For}\quad \eta=0: \qquad F(0,\tau)=0,\quad \frac{\partial F}{\partial \eta}(0,\tau)=0,\quad G(0,\tau)=0,\\ &\text{For}\quad \eta\to\infty: \qquad \frac{\partial F}{\partial \eta}(\eta,\tau)\to 0,\quad G(\eta,\tau)\to 0.\end{aligned} \tag{23}$$

To investigate the stability of steady flow solutions $f_0(\eta)$ and $\theta_0(\eta)$, set $\tau=0$ in Eqs. (21)−(23). Hence $F(\eta,\tau)=F_0(\eta)$ and $G(\eta,\tau)=G_0(\eta)$ represents the initial growth or decay of the solution. In this regard, the following linear eigenvalue problem is to be solved

$$\frac{A_1}{A_2}F_0'''+\left(\gamma-2f_0'\right)F_0'\ +f_0''\,F_0+f_0F_0''-\frac{A_3}{A_2}M\,F_0'\ =0\,, \tag{24}$$

$$\left(A_4+R\right)G_0''\ +A_5\,P_r\left(F_0\,\theta_0'+f_0G_0'\ +\gamma G_0\right)=0\,, \tag{25}$$

with BCs:

$$\begin{aligned}&\text{For}\quad \eta=0: \qquad F_0(0)=0,\quad F_0'\ (0)=0,\quad G_0(0)=0,\\ &\text{For}\quad \eta\to\infty: \qquad F_0'(\eta)\to 0,\quad G_0(\eta)\to 0\,.\end{aligned} \tag{26}$$

By finding the smallest eigenvalues, stability of the dual solutions is applied for certain values of parameters like: λ, M, P_r and R. Harris et al. [26] stated in their study that to calculate the eigenvalues, an extra boundary condition is used. For this purpose, $F_0''\,(0)=1$ a condition is applied to the problem and then it is solved using the bvp4c function in Matlab software.

4. Least square method

The Weighted Residual technique such as the Least square method is an approximation technique that gives the most useable procedure that applies to nonlinear dynamical models. The central idea of this method is to obtain an estimated solution of the differential equation.

Consider a differential equation

$$D(\tilde{F})=\tilde{f}\ , \tag{27}$$

subjected to the boundary conditions

$$B_j\tilde{F}=\tilde{g}_j\,. \tag{28}$$

In order to discover an estimated solution to the given problem, consider a linear combination set (linearly independent) of a basis functions. That is,

$$\hat{F} = \tilde{F}_0 + \sum_{j=1}^{m} c_j \tilde{\phi}_j \ . \tag{29}$$

Here $\tilde{F}_0$ is selected in a manner that the boundary conditions are satisfied, exactly if possible. $\tilde{\phi}_j$ are the linearly independent functions, also called trial functions, and are supposed to be known. The coefficients c_j are unknowns and can be obtained by solving a system of equations.

When substituted Eq. (29) in Eq. (27), it will not satisfy the equation. Hence an error or residual $\tilde{R}$, which is a continuous function of spatial coordinates, exists and is written as

$$\tilde{R} = D(\hat{F}) - \tilde{f} \neq 0 \, . \tag{30}$$

In one spatial coordinate, the approximating functions may be the trigonometric functions or the polynomials of the form

$$\tilde{\phi}_j(\varepsilon) = \varepsilon^{j-1} \text{ or } \tilde{\phi}_j(\eta) = sinj\pi\varepsilon \, . \tag{31}$$

The notion in the least square method is to make the error (residual) equal to zero over the entire domain (say) X in an average sense.

$$\int_X \tilde{R}(\varepsilon) W_j(\varepsilon) \, d\varepsilon = 0 \, , \quad j = 1, 2, 3, ...m \, . \tag{32}$$

Where weight functions and the unknown coefficients c_j are exactly equal. We take the sum of the squares of residuals rather than the sum of residuals. So, this sum is minimized and given as

$$E = \int_X \tilde{R}(\varepsilon) \tilde{R}(\varepsilon) \, d\varepsilon = \int_X \tilde{R}^2(\varepsilon) \, d\, \varepsilon \, . \tag{33}$$

Now to get the minimum of the given function, the derivative of Eq. (33) concerning the unknown coefficients c_j is set to be zero. That is,

$$\frac{\partial E}{\partial c_j} = 2 \int_X \tilde{R}(\varepsilon) \frac{\partial \tilde{R}}{\partial c_j} d\, \varepsilon = 0 \, , \qquad j = 1, 2, 3, ...m \, . \tag{34}$$

Comparing Eq. (34) with Eq. (32), the weight functions become

$$W_j = 2 \frac{\partial \tilde{R}}{\partial c_j} \, . \tag{35}$$

Since the coefficient ‘2’ can be ignored as it vanishes in the given equation. Thus, the weight functions are given by

$$W_j = \frac{\partial \tilde{R}}{\partial c_j}. \tag{36}$$

5. Solutions

The domain of the problem under consideration is $[0,\infty]$. To convert this domain into a finite domain $[0,1]$, a transformation $\varepsilon = \eta/\eta_\infty$ is needed [46]. ε is called a similarity variable and η_∞ indicates the edge of the boundary layer or physical infinity. Using the above transformation, BVP has given in Eq. (8)−(9) with Eq. (12} now becomes:

$$\frac{A_1}{A_2}\frac{d^3 f(\varepsilon)}{d\varepsilon^3} + \eta_\infty^3 - \eta_\infty \left(\frac{d f(\varepsilon)}{d\varepsilon}\right)^2 + \eta_\infty\, f(\varepsilon)\frac{d^2 f(\varepsilon)}{d\varepsilon^2} - M\,\frac{A_3}{A_2}\left(\eta_\infty^2 \frac{d f(\varepsilon)}{d\varepsilon} - \eta_\infty^3\right) = 0, \tag{37}$$

$$\left(A_4 + R\right)\frac{d^2\theta(\varepsilon)}{d\varepsilon^2} + \eta_\infty\, A_5\, P_r\, f(\varepsilon)\,\frac{d\theta(\varepsilon)}{d\varepsilon} = 0. \tag{38}$$

BCs:

$$\begin{aligned} &\text{For} \quad \varepsilon = 0: \qquad f(\varepsilon) = 0, \qquad \frac{d f(\varepsilon)}{d\varepsilon} = \eta_\infty\,\lambda, \qquad \theta(\varepsilon) = 1, \\ &\text{For} \quad \varepsilon = 1: \qquad \frac{d f(\varepsilon)}{d\varepsilon} = \eta_\infty, \qquad \theta(\varepsilon) = 0. \end{aligned} \tag{39}$$

Using Eq. (29), trial functions satisfying the boundary conditions given in Eq. (39) take the form:

$$\begin{aligned} &\hat{f}(\eta) = \eta_\infty \lambda\,\varepsilon + \frac{\eta_\infty(1-\lambda)}{2}\varepsilon^2 + c_1\left(\frac{-3\varepsilon^2}{2} + \varepsilon^3\right) + c_2\left(\frac{-4\varepsilon^3}{3} + \varepsilon^4\right) + c_3\left(\frac{-5\varepsilon^4}{4} + \varepsilon^5\right) + c_4\left(\frac{-6\varepsilon^5}{5} + \varepsilon^6\right), \\ &\hat{\theta}(\eta) = 1 - \varepsilon + c_5(-\varepsilon + \varepsilon^2) + c_6(-\varepsilon + \varepsilon^3). \end{aligned} \tag{40}$$

Substitution of Eq. (40) in Eqs. (37)−(38) give the two residuals:

$$\tilde{R}_1(c_1-c_4,\varepsilon)=6c_1+30c_3\,\varepsilon(2\varepsilon-1)+8c_2(3\varepsilon-1)+24c_4\varepsilon^2(5\varepsilon-3)-\frac{A_3}{A_1}M\eta_\infty^2(\varepsilon-1)(3c_1\varepsilon+4c_2\varepsilon^2$$
$$+5c_3\varepsilon^3+6c_4\varepsilon^4+\eta_\infty-\eta_\infty\lambda)+\frac{A_2}{A_1}(\eta_\infty^3+\frac{\eta_\infty\,\varepsilon}{60}(20c_3\varepsilon^3-24c_4\varepsilon^3+30c_4\varepsilon^4-15c_3\varepsilon^2+4c_2\varepsilon(3\varepsilon-2)$$
$$+c_1(6\varepsilon-3)+\eta_\infty-\eta_\infty\lambda)(60c_3\varepsilon^4-72c_4\varepsilon^4+60c_4\varepsilon^5-75c_3\varepsilon^3+30c_1\varepsilon(2\varepsilon-3)+20c_2\varepsilon^2(3\varepsilon-4)$$
$$+30\eta_\infty\varepsilon+60\eta_\infty\lambda-30\eta_\infty\lambda\,\varepsilon)-\eta_\infty(3c_1\varepsilon(\varepsilon-1)+4c_2\varepsilon^2(\varepsilon-1)-5c_3\varepsilon^3+5c_3\varepsilon^4-6c_4\varepsilon^4+6c_4\varepsilon^5$$
$$+\eta_\infty\varepsilon+\eta_\infty\lambda-\eta_\infty\lambda\varepsilon)^2),$$

and

$$\tilde{R}_2(c_1-c_6,\varepsilon)=2c_5+6c_6\,\varepsilon+\frac{A_5P_r\eta_\infty}{(A_4+R)}\left(-1+c_5(2\varepsilon-1)+c_6(3\varepsilon^2-1)\right)\times$$
$$\left(c_1\left(\varepsilon^3-\frac{3\varepsilon^2}{2}\right)+c_2\left(\varepsilon^4-\frac{4\varepsilon^3}{3}\right)+c_3\left(\varepsilon^5-\frac{5\varepsilon^4}{4}\right)+c_4\left(\varepsilon^6-\frac{6\varepsilon^5}{5}\right)+\frac{\eta_\infty\varepsilon^2(1-\lambda)}{2}+\eta_\infty\lambda\,\varepsilon\right).$$

Using Eq. (36), the weight functions are obtained:

$$W_1=\frac{\partial\tilde{R}_1}{\partial c_1},\quad W_2=\frac{\partial\tilde{R}_1}{\partial c_2},\quad W_3=\frac{\partial\tilde{R}_1}{\partial c_3},\quad W_4=\frac{\partial\tilde{R}_1}{\partial c_4},\quad W_5=\frac{\partial\tilde{R}_2}{\partial c_5},\quad W_6=\frac{\partial\tilde{R}_2}{\partial c_6}.\qquad(41)$$

Substitution of the weights along with the residuals in Eq. (32) gives a system of six nonlinear equations in six unknowns (c_1-c_6). By applying Newton's method [34], the unknowns (c_1-c_6) are evaluated. Finally, $\hat{f}(\eta)$ and $\hat{\theta}(\eta)$ for dual solutions are obtained in the following forms:

For Al_2O_3-ZnO / kerosene hybrid nanofluid:

The first solution ($\lambda=-1.2,\ P_r=1,\ R=0.5,\ \phi_1=\phi_2=0.1$ and $M=0.01$)

$$\hat{f}(\varepsilon)=-7.2\varepsilon+6.6\varepsilon^2+1.90699\left(\varepsilon^3-\frac{3\varepsilon^2}{2}\right)-12.76200\left(\varepsilon^4-\frac{4\varepsilon^3}{3}\right)+6.76692\left(\varepsilon^5-\frac{5\varepsilon^4}{4}\right)$$
$$-0.10759\left(\varepsilon^6-\frac{6\varepsilon^5}{5}\right),\qquad(42)$$

$$\hat{\theta}(\varepsilon)=1-\varepsilon-1.20773(\varepsilon^2-\varepsilon)+0.31052(\varepsilon^3-\varepsilon).$$

The second solution ($\lambda=-1.2,\ P_r=1,\ R=0.5,\ \phi_1=\phi_2=0.1$ and $M=0.01$)

$$\hat{f}(\varepsilon) = -12\varepsilon + 11\varepsilon^2 - 33.9765\left(\varepsilon^3 - \frac{3\varepsilon^2}{2}\right) + 31.434\left(\varepsilon^4 - \frac{4\varepsilon^3}{3}\right) - 0.564293\left(\varepsilon^5 - \frac{5\varepsilon^4}{4}\right) - 7.57447\left(\varepsilon^6 - \frac{6\varepsilon^5}{5}\right), \quad (43)$$

$$\hat{\theta}(\varepsilon) = 1 - \varepsilon + 2.82165(\varepsilon^2 - \varepsilon) - 0.889414(\varepsilon^3 - \varepsilon).$$

For ZnO / kerosene nanofluid:

The first solution ($\lambda = -1.2$, $P_r = 1$, $R = 0.5$, $\phi_1 = 0$, $\phi_2 = 0.1$ and $M = 0.01$)

$$\hat{f}(\varepsilon) = -7.2\varepsilon + 6.6\varepsilon^2 + 1.92462\left(\varepsilon^3 - \frac{3\varepsilon^2}{2}\right) - 13.6033\left(\varepsilon^4 - \frac{4\varepsilon^3}{3}\right) + 7.68807\left(\varepsilon^5 - \frac{5\varepsilon^4}{4}\right) - 0.355034\left(\varepsilon^6 - \frac{6\varepsilon^5}{5}\right), \quad (44)$$

$$\hat{\theta}(\varepsilon) = 1 - \varepsilon - 1.3207(\varepsilon^2 - \varepsilon) + 0.42405(\varepsilon^3 - \varepsilon).$$

The second solution ($\lambda = -1.2$, $P_r = 1$, $R = 0.5$, $\phi_1 = 0$, $\phi_2 = 0.1$ and $M = 0.01$)

$$\hat{f}(\varepsilon) = -12\varepsilon + 11\varepsilon^2 + 2.62652\left(\varepsilon^3 - \frac{3\varepsilon^2}{2}\right) - 66.9822\left(\varepsilon^4 - \frac{4\varepsilon^3}{3}\right) + 90.6693\left(\varepsilon^5 - \frac{5\varepsilon^4}{4}\right) - 36.0774\left(\varepsilon^6 - \frac{6\varepsilon^5}{5}\right), \quad (45)$$

$$\hat{\theta}(\varepsilon) = 1 - \varepsilon - 2.66095(\varepsilon^2 - \varepsilon) + 1.89097(\varepsilon^3 - \varepsilon).$$

For Al_2O_3 / kerosene nanofluid:

The first solution ($\lambda = -1.2$, $P_r = 1$, $R = 0.5$, $\phi_1 = 0.1$, $\phi_2 = 0$ and $M = 0.01$)

$$\hat{f}(\varepsilon) = -7.2\varepsilon + 6.6\varepsilon^2 + 1.95054\left(\varepsilon^3 - \frac{3\varepsilon^2}{2}\right) - 11.3837\left(\varepsilon^4 - \frac{4\varepsilon^3}{3}\right) + 5.24249\left(\varepsilon^5 - \frac{5\varepsilon^4}{4}\right) + 0.30265\left(\varepsilon^6 - \frac{6\varepsilon^5}{5}\right), \quad (46)$$

$$\hat{\theta}(\varepsilon) = 1 - \varepsilon - 0.932766(\varepsilon^2 - \varepsilon) + 0.010247(\varepsilon^3 - \varepsilon).$$

The second solution ($\lambda = -1.2$, $P_r = 1$, $R = 0.5$, $\phi_1 = 0.1$, $\phi_2 = 0$ and $M = 0.01$)

$$\hat{f}(\varepsilon) = -12\varepsilon + 11\varepsilon^2 - 23.9419\left(\varepsilon^3 - \frac{3\varepsilon^2}{2}\right) - 3.15035\left(\varepsilon^4 - \frac{4\varepsilon^3}{3}\right) + 40.1955\left(\varepsilon^5 - \frac{5\varepsilon^4}{4}\right) - 23.6605\left(\varepsilon^6 - \frac{6\varepsilon^5}{5}\right), \quad (47)$$

$$\hat{\theta}(\varepsilon) = 1 - \varepsilon + 2.29968(\varepsilon^2 - \varepsilon) - 0.610238(\varepsilon^3 - \varepsilon).$$

6. Results and Discussion

An analytical method namely the Least square method [45] is applied to a nonlinear system of ODEs. Newton's method [44] is used to linearize the system. Dual solutions are obtained for $Al_2O_3 - ZnO$ / kerosene hybrid nanofluid, Al_2O_3 / kerosene nanofluid, and ZnO / kerosene nanofluid. Furthermore, a stability analysis is applied to the time-dependent problem to determine a reliable solution. The comparison of three distinct fluids such as $Al_2O_3 - ZnO$ / kerosene hybrid nanofluid, Al_2O_3 / kerosene nanofluid, and ZnO / kerosene nanofluid is also made and displayed in graphs. Dual solutions occur for a shrinking case $(\lambda < 0)$ which is displayed in the methodology section. For the validation of numerical outcomes, a comparison of skin friction coefficient is done with the work of Wang [2] and presented in Table 3. This table depicts that the numerical findings are in good agreement, where the values in brackets specify the second solution.

The results of the coefficient of skin friction and the local Nusselt number in graphical form are presented in Figs. 2 and 3 to give a range of dual solutions. In these figures, the solid lines correspond to 1st solution and dotted lines correspond to 2nd solution. The main focus of this paper is to implement stability analysis on the problem to check stable or physically reliable solutions. For this purpose, Tables 4 and 5 show the least eigenvalues which are found for distinct values of parameters. Positive eigenvalues correspond to the stable solution (1st solution) due to initial decline in solution and negative eigenvalues correspond to an unstable solution (2nd solution) due to initial progress of disturbance in solution. To validate the results, a comparison is made with the published work of Awaludin et al. [28] for the eigenvalues with $M = R = \phi_1 = \phi_2 = 0$ and depicted in Table 4. Clearly, this table shows that both results are in good agreement. Processing

time is also noted and presented in this table to ensure that the Least square method converges fast as other analytical techniques such as the Homotopy analysis method (HAM).

Table 5 displays the calculated eigenvalues of the present BVP for both solutions under the effects of MHD and radiation. This table gives the comparison of three different fluids. The smallest positive and smallest negative eigenvalues are found to give 1st stable and 2nd unstable solution as described earlier. From this table, it is noticed that the increment in the values of parameters results from higher eigenvalues.

Figs. 2 and 3 depict the plots of the coefficient of skin friction and the local Nusselt number against λ for dual solutions with three distinct fluids when $P_r = 1, M = 0.1$ and $R = 0.5$. It is noticed that the coefficient of skin friction and the local Nusselt number for $Al_2O_3 - ZnO$ / kerosene hybrid nanofluid $(\phi_1 = \phi_2 = 0.1)$ is higher than Al_2O_3 / kerosene nanofluid $(\phi_1 = 0.1, \phi_2 = 0)$ and lower than ZnO / kerosene nanofluid $(\phi_1 = 0, \phi_2 = 0.1)$. A significant change is observed in 1st solution whereas a very small variation is observed in 2nd solution. From Fig. 2, it is noted that values of the coefficient of skin friction increases for $\lambda < 1$ up to a certain value and then begin to decrease after this value. Fig. 3 illustrates that the rate of heat transfer for the first solution is enhanced by increasing λ while the second solution is very close to zero. The dual solutions range for $Al_2O_3 - ZnO$ / kerosene hybrid nanofluid is $-1.3172 < \lambda < -1.13$, Al_2O_3 / kerosene nanofluid is $-1.3312 < \lambda < -1.13$ and ZnO / kerosene nanofluid is $-1.3188 < \lambda < -1.13$. Hence a larger range of dual solutions is observed with Al_2O_3 / kerosene nanofluid.

The comparison of $Al_2O_3 - ZnO$ / kerosene hybrid nanofluid $(\phi_1 = \phi_2 = 0.1)$, Al_2O_3 / kerosene nanofluid $(\phi_1 = 0, \phi_2 = 0.1)$, and ZnO / kerosene nanofluid $(\phi_1 = 0, \phi_2 = 0.1)$ with $P_r = 1, M = 0.2, \lambda = -1.35$ and $R = 0.5$ is shown in Figs. 4(a, b) and 5(a, b), where Figs. 4a and 4b display the graph of a velocity profile $f'(\eta)$ for the first and second solution, respectively whereas Fig. 5a represents the first and Fig.5b represents the second solution for the temperature profile $\theta(\eta)$. It is determined from Fig. 4(a,b) that the velocity profile $f'(\eta)$ becomes higher with ZnO / kerosene nanofluid and lower with Al_2O_3 / kerosene nanofluid while it lies in between for hybrid nanofluid. And for $\theta(\eta)$, an opposite trend is noticed in Figs 5a and 5b such that the

temperature profile $\theta(\eta)$ for hybrid nanofluid is smaller than Al_2O_3 / kerosene nanofluid but larger than ZnO / kerosene nanofluid.

Figs. 6 and 7 show the impacts of velocity ratio parameter λ on $f'(\eta)$ and $\theta(\eta)$, respectively for $Al_2O_3 - ZnO$ / kerosene hybrid nanofluid $(\phi_1 = \phi_2 = 0.1)$, Al_2O_3 / kerosene nanofluid $(\phi_1 = 0.1, \phi_2 = 0)$, and ZnO / kerosene nanofluid $(\phi_1 = 0, \phi_2 = 0.1)$ with $P_r = 1$, $M = 0.05$ and $R = 0.5$. It is examined from Fig. 6 that the velocity profile increases λ while Fig. 7 depicts that the temperature profile decreases when λ is increased. It is concluded from these figures that the behavior of λ is the same for all three types of fluid.

Fig. 8 displays the influence of radiation parameter R on $\theta(\eta)$ in case of hybrid nanofluid for dual solutions at $\phi_1 = \phi_2 = 0.1, P_r = 1, \lambda = -1.25$ and $M = 0.1$. It is observed that the increment in the values of radiation parameter increases $\theta(\eta)$ for 1st solution but in the case of 2nd solution $\theta(\eta)$ decreases initially and then after a certain point, it begins to increase.

Table 3 Comparison of coefficient of skin friction $f''(0)$ with $R = M = \phi_1 = \phi_2 = 0$.

λ	Wang [2]	Present study
1	0	0
0.5	0.71330	0.71330
0	1.23258	1.23258
−0.25	1.40224	1.40224
−0.5	1.49567	1.49567
−0.75	1.48930	1.48930
−1	1.32882 [0]	1.32880 [0]
−1.15	1.08223 [0.11670]	1.08220 [0.11670]

Table 4: Comparison for smallest eigenvalues γ with $M = R = \phi_1 = \phi_2 = 0$ and $P_r = 1$.

λ	Awaludin et al. [28]		Present study		CPU time (s)
	1st solution	2nd solution	1st solution	2nd solution	
−1	1.3690	---	1.3690	---	22.801
−1.1	1.0463	−0.8437	1.0463	−0.8437	23.701
−1.2	0.5780	−0.5173	0.5780	−0.5173	23.167

−1.24	0.2121	−0.2036	0.2121	−0.2036	23.366
−1.245	0.1030	−0.1010	0.1030	−0.1010	23.790
−1.246	0.0622	−0.0614	0.0622	−0.0614	23.303

Table 5: Comparison of smallest eigenvalues γ for three fluids with $M = 0.1, R = 0.5$ and $P_r = 1$

	$Al_2O_3 - ZnO$ / kerosene $(\phi_1 = \phi_2 = 0.1)$		Al_2O_3 / kerosene $(\phi_1 = 0.1, \phi_2 = 0)$		ZnO / kerosene $(\phi_1 = 0, \phi_2 = 0.1)$	
λ	1st solution	2nd solution	1st solution	2nd solution	1st solution	2nd solution
−1.18	1.0182	−0.8281	1.0723	−0.8614	1.0247	−0.8323
−1.20	0.9381	0.7787	0.9963	−0.8152	0.9457	−0.7821
−1.21	0.8952	−0.7501	0.9562	−0.7907	0.9032	−0.7551
−1.23	0.8059	−0.6874	0.8712	−0.7344	0.8131	−0.6931
−1.25	0.7033	−0.6141	0.8724	−0.6681	0.7982	−0.6215
−1.27	0.5851	−0.5237	0.6713	−0.5901	0.5961	−0.5324
−1.29	0.4416	−0.4053	0.5472	−0.4932	0.4551	−0.4170
−1.30	0.3480	−0.3268	0.4756	−0.4331	0.3651	−0.3410
−1.31	0.2234	−0.2141	0.3892	−0.3612	0.2486	−0.2373

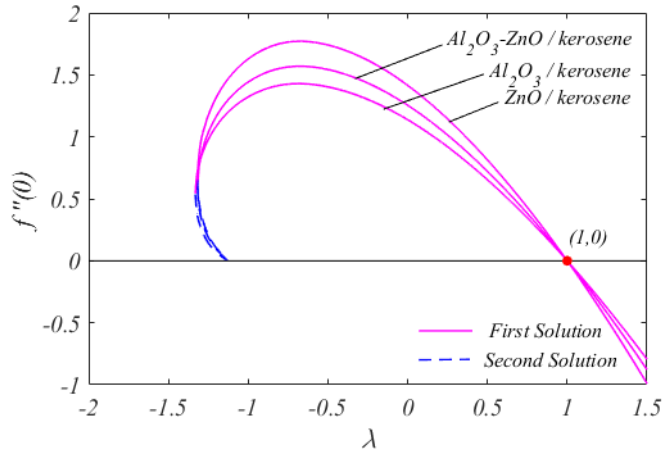

Fig. 2. Comparison of three distinct fluids for $f''(0)$.

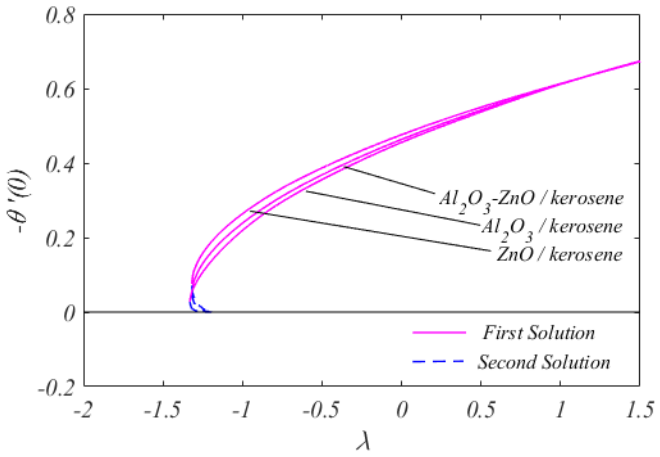

Fig. 3. Comparison of three distinct fluids for $-\theta'(0)$.

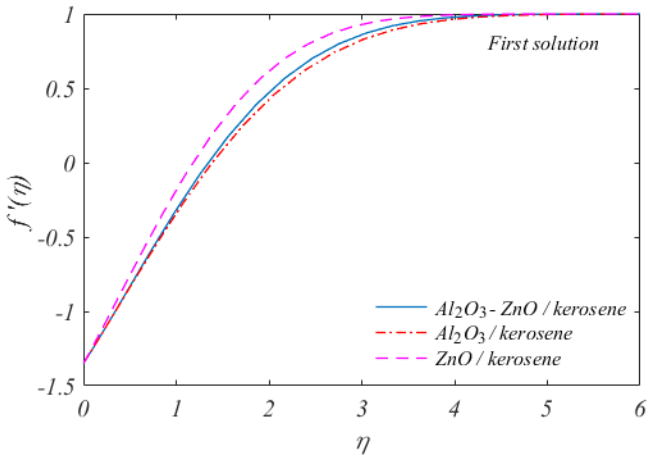

Fig. 4a. Comparison of three distinct fluids for 1st solution of $f'(\eta)$.

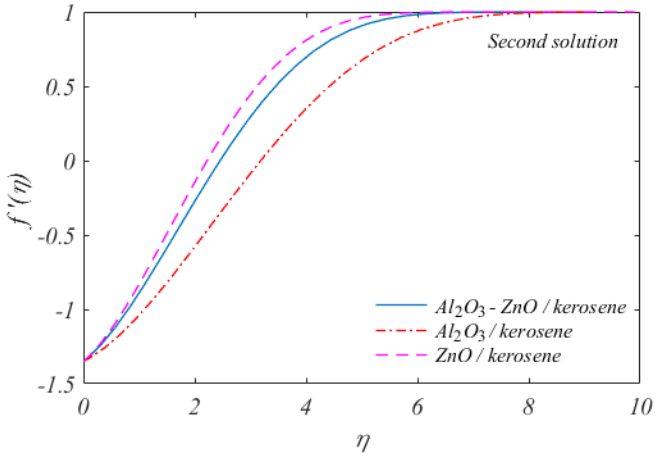

Fig. 4b. Comparison of three distinct fluids for 2nd solution of $f'(\eta)$.

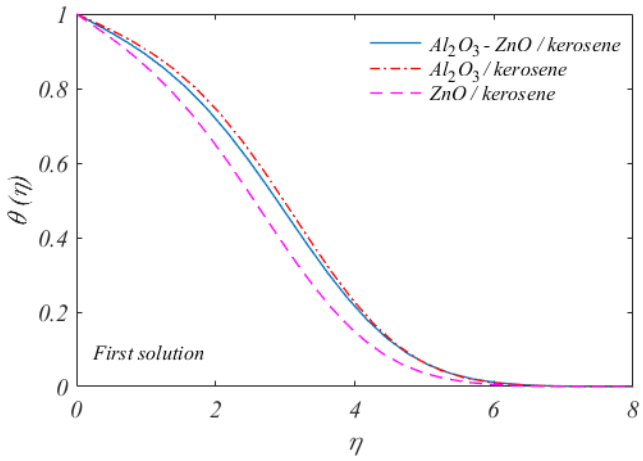

Fig. 5a. Comparison of three distinct fluids for 1st solution of $\theta(\eta)$.

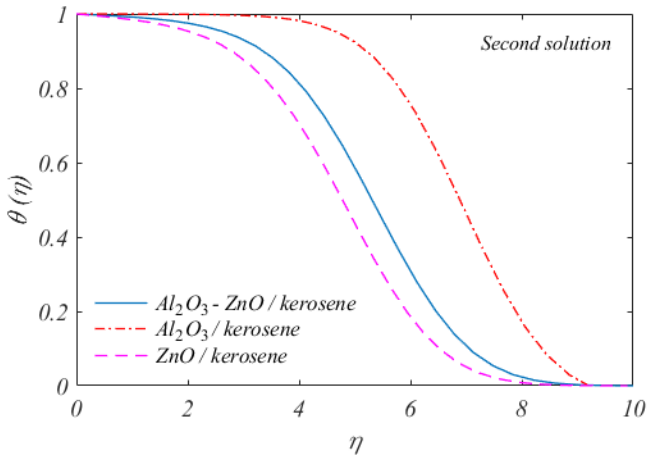

Fig. 5b. Comparison of three distinct fluids for 2nd solution of $\theta(\eta)$.

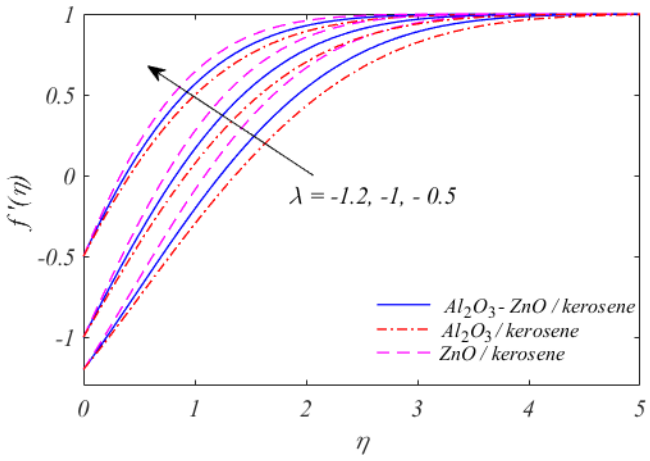

Fig. 6. Variations of λ on $f'(\eta)$ for three distinct fluids.

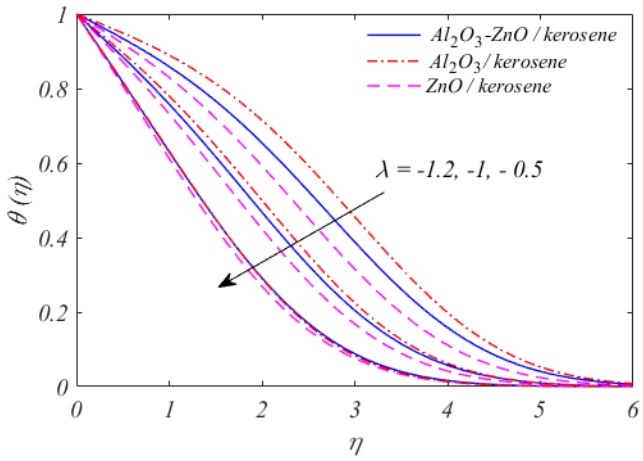

Fig. 7. Variations of λ on $\theta(\eta)$ for three distinct fluids.

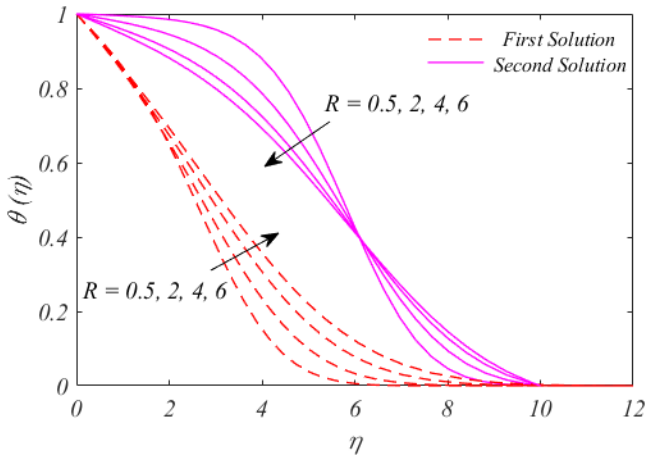

Fig. 8. Variations of radiation parameter R on $\theta(\eta)$ for hybrid nanofluid.

7. Conclusion

The BVP presented in Eqs. (8)–(9) and Eq. (12) are solved analytically using the Least square method (LSM). This analytical method is so simple and easy that it can be applied to any BVP. This method takes less time for finding solutions than the homotopy analysis method (HAM). Dual solutions are computed with the influence of MHD and radiation for three different fluids and the range of dual solutions is larger with Al_2O_3 / kerosene nanofluid. Moreover, stability analysis is applied to check stable or physically reliable solutions. The eigenvalues are evaluated for various parameters, where the positive eigenvalues are related to stable solutions and negative eigenvalues

are related to the unstable solution. Higher eigenvalues are found with the effects of MHD. $\theta(\eta)$ enhances with the enhancement of radiation parameter R for 1st solution but declines initially for 2nd solution and then after a certain value, it begins to increase.

References

[1] Miklavčič, M. and Wang, C. (2006) Viscous flow due to a shrinking sheet. *Quarterly of Applied Mathematics, 64* (2), 283-290.

[2] Wang, C. Y. (2008) Stagnation flow towards a shrinking sheet. *International Journal of Non-Linear Mechanics, 43* (5), 377-382.

[3] Ishak, A., Lok, Y. Y. and Pop, I. (2010) Stagnation-point flow over a shrinking sheet in a micropolar fluid. *Chemical Engineering Communications, 197* (11), 1417-1427.

[4] Fang, T. and Zhang, J. (2010) Thermal boundary layers over a shrinking sheet: an analytical solution. *Acta Mechanica, 209* (3), 325-343.

[5] Lok, Y. Y., Ishak, A. and Pop, I. (2011) MHD stagnation-point flow towards a shrinking sheet. *International Journal of Numerical Methods for Heat & Fluid Flow*.

[6] Bhattacharyya, K. and Layek, G. C. (2011) Effects of suction/blowing on steady boundary layer stagnation-point flow and heat transfer towards a shrinking sheet with thermal radiation. *International Journal of Heat and Mass Transfer, 54* (1-3), 302-307.

[7] Bhattacharyya, K., Mukhopadhyay, S. and Layek, G. C. (2011) Slip effects on boundary layer stagnation-point flow and heat transfer towards a shrinking sheet. *International Journal of Heat and Mass Transfer, 54* (1-3), 308-313.

[8] Soid, S. K., Ishak, A. and Pop, I. (2015) MHD stagnation point flow over a stretching/shrinking sheet. In *2015 International Symposium on Mathematical Sciences and Computing Research*, 355-360.

[9] Abd El-Aziz, M. (2016) Dual solutions in hydromagnetic stagnation point flow and heat transfer towards a stretching/shrinking sheet with non-uniform heat source/sink and variable surface heat flux. *Journal of the Egyptian Mathematical Society, 24* (3), 479-486.

[10] Rao, M. E. and Sreenadh, S. (2017) MHD boundary layer flow of Jeffrey fluid over a stretching/shrinking sheet through porous medium. *Global Journal of Pure and Applied Mathematics, 13* (8), 3985-4001.

[11] Maxwell, J. C. (1873) *A treatise on electricity and magnetism* (Vol. 1). Clarendon Press.

[12] Choi, S. U. and Eastman, J. A. (1995) *Enhancing thermal conductivity of fluids with nanoparticles* (No. ANL/MSD/CP-84938; CONF-951135-29). Argonne National Lab., IL (United States).

[13] Mahian, O., Kolsi, L., Amani, M., Estellé, P., Ahmadi, G., Kleinstreuer, C., ... and Pop, I. (2019) Recent advances in modeling and simulation of nanofluid flows-Part I: Fundamentals and theory. *Physics reports*, *790*, 1-48.

[14] Maleki, H., Alsarraf, J., Moghanizadeh, A., Hajabdollahi, H. and Safaei, M. R. (2019) Heat transfer and nanofluid flow over a porous plate with radiation and slip boundary conditions. *Journal of Central South University*, *26* (5), 1099-1115.

[15] Ahmadi, A. A., Arabbeiki, M., Ali, H. M., Goodarzi, M., and Safaei, M. R. (2020) Configuration and optimization of a minichannel using water–alumina nanofluid by non-dominated sorting genetic algorithm and response surface method. *Nanomaterials*, *10* (5), 901.

[16] Safaei, M. R., Tlili, I., Gholamalizadeh, E., Abbas, T., Alkanhal, T. A., Goodarzi, M. and Dahari, M. (2021) Thermal analysis of a binary base fluid in pool boiling system of glycol–water alumina nano-suspension. *Journal of Thermal Analysis and Calorimetry*, *143* (3), 2453-2462.

[17] Suresh, S., Venkitaraj, K. P. and Selvakumar, P. (2011) Synthesis, Characterisation of Al2O3-Cu Nano composite powder and water based nanofluids. In *Advanced Materials Research*, *328*, 1560-1567. Trans Tech Publications Ltd.

[18] Suresh, S., Venkitaraj, K. P., Selvakumar, P. and Chandrasekar, M. (2011) Synthesis of Al2O3–Cu/water hybrid nanofluids using two step method and its thermo physical properties. *Colloids and Surfaces A: Physicochemical and Engineering Aspects*, *388* (1-3), 41-48.

[19] Devi, S. S. U. and Devi, S. A. (2016) Numerical investigation of three-dimensional hybrid Cu–Al2O3/water nanofluid flow over a stretching sheet with effecting Lorentz force subject to Newtonian heating. *Canadian Journal of Physics*, *94* (5), 490-496.

[20] Khashi'ie, N. S., Arifin, N. M., Pop, I., Nazar, R., Hafidzuddin, E. H. and Wahi, N. (2020) Three-dimensional hybrid nanofluid flow and heat transfer past a permeable stretching/shrinking sheet with velocity slip and convective condition. *Chinese Journal of Physics*, *66*, 157-171.

[21] Zainal, N. A., Nazar, R., Naganthran, K. and Pop, I. (2020) Unsteady three-dimensional MHD non-axisymmetric Homann stagnation point flow of a hybrid nanofluid with stability analysis. *Mathematics*, *8* (5), 784.

[22] Waini, I., Ishak, A. and Pop, I. (2020) MHD flow and heat transfer of a hybrid nanofluid past a permeable stretching/shrinking wedge. *Applied Mathematics and Mechanics*, *41* (3), 507-520.

[23] Merkin, J. H. (1986) On dual solutions occurring in mixed convection in a porous medium. *Journal of engineering Mathematics*, *20* (2), 171-179.

[24] Weidman, P. D., Kubitschek, D. G. and Davis, A. M. J. (2006) The effect of transpiration on self-similar boundary layer flow over moving surfaces. *International journal of engineering science*, *44* (11-12), 730-737.

[25] Merrill, K., Beauchesne, M., Previte, J., Paullet, J. and Weidman, P. (2006) Final steady flow near a stagnation point on a vertical surface in a porous medium. *International journal of heat and mass transfer*, *49* (23-24), 4681-4686.

[26] Harris, S. D., Ingham, D. B. and Pop, I. (2009) Mixed convection boundary-layer flow near the stagnation point on a vertical surface in a porous medium: Brinkman model with slip. *Transport in Porous Media*, *77* (2), 267-285.

[27] Mahapatra, T. R. and Nandy, S. K. (2013) Stability of dual solutions in stagnation-point flow and heat transfer over a porous shrinking sheet with thermal radiation. *Meccanica*, *48* (1), 23-32.

[28] Awaludin, I. S., Weidman, P. D. and Ishak, A. (2016) Stability analysis of stagnation-point flow over a stretching/shrinking sheet. *AIP Advances*, *6* (4), 045308.

[29] Hamid, M., Usman, M., Khan, Z. H., Ahmad, R. and Wang, W. (2019) Dual solutions and stability analysis of flow and heat transfer of Casson fluid over a stretching sheet. *Physics Letters A*, *383* (20), 2400-2408.

[30] Waini, I., Ishak, A. and Pop, I. (2019) Unsteady flow and heat transfer past a stretching/shrinking sheet in a hybrid nanofluid. *International Journal of Heat and Mass Transfer*, *136*, 288-297.

[31] Zainal, N. A., Nazar, R., Naganthran, K. and Pop, I. (2021) Stability analysis of MHD hybrid nanofluid flow over a stretching/shrinking sheet with quadratic velocity. *Alexandria Engineering Journal*, *60* (1), 915-926.

[32] Zhang, L., Nazar, T., Bhatti, M. M. and Michaelides, E. E. (2021) Stability analysis on the kerosene nanofluid flow with hybrid zinc/aluminum-oxide (ZnO-Al2O3) nanoparticles under Lorentz force. *International Journal of Numerical Methods for Heat & Fluid Flow*.

[33] Nayfeh, A. H. (2008) *Perturbation methods*. John Wiley & Sons.

[34] Khan, Z. H., Gul, R. and Khan, W. A. (2008) Effect of variable thermal conductivity on heat transfer from a hollow sphere with heat generation using homotopy perturbation method. In *Heat Transfer Summer Conference*, 48470, 301-309.

[35] Beléndez, A., Pascual, C., Neipp, C., Beléndez, T. and Hernández, A. (2008) An equivalent linearization method for conservative nonlinear oscillators. *International Journal of Nonlinear Sciences and Numerical Simulation*, *9* (1), 9-18.

[36] He, J. H. (2002) Modified Lindstedt–Poincare methods for some strongly non-linear oscillations: Part I: expansion of a constant. *International Journal of Non-Linear Mechanics*, *37* (2), 309-314.

[37] Zhou, J. K. (1986) Differential transformation and its applications for electrical circuits.

[38] Herişanu, N. and Marinca, V. (2012) Optimal homotopy perturbation method for a non-conservative dynamical system of a rotating electrical machine. *Zeitschrift für Naturforschung A*, *67* (8-9), 509-516.

[39] Bouaziz, M. N. and Aziz, A. (2010) Simple and accurate solution for convective–radiative fin with temperature dependent thermal conductivity using double optimal linearization. *Energy Conversion and Management*, *51* (12), 2776-2782.

[40] Hatami, M. and Ganji, D. D. (2013) Heat transfer and flow analysis for SA-TiO2 non-Newtonian nanofluid passing through the porous media between two coaxial cylinders. *Journal of molecular liquids*, *188*, 155-161.

[41] Hatami, M. and Ganji, D. D. (2014) Thermal and flow analysis of microchannel heat sink (MCHS) cooled by Cu–water nanofluid using porous media approach and least square method. *Energy Conversion and management*, *78*, 347-358.

[42] Hamid, M., Usman, M., Zubair, T., Haq, R. U. and Wang, W. (2018) Shape effects of MoS2 nanoparticles on rotating flow of nanofluid along a stretching surface with variable thermal conductivity: A Galerkin approach. *International Journal of Heat and Mass Transfer*, *124*, 706-714.

[43] Sparrrow, E. M. and Cess, R. D. (1978) Radiation Heat Transfer, Washington, DC, USA: Hemisphere.

[44] Burden, R. L. and Faires, J. D. (1991) Numerical Analysis, fourth ed., *International Thomson Publishing*.

[45] Portela, A. and Charafi, A. (2002) Finite Elements using Maple, *Springer-Verlag Berlin Heidelberg*.

[46] Mustafa, I., Abbas, Z., Arif, A., Javed, T. and Ghaffari, A. (2020) Stability analysis for multiple solutions of boundary layer flow towards a shrinking sheet: analytical solution by using least square method. *Physica A: Statistical Mechanics and its Applications*, *540*, 123028.